Reviews

A Journey from 12-Vertex to 14-Vertex Carboranes and to 15-Vertex Metallacarboranes

Liang Deng and Zuowei Xie*

Department of Chemistry, The Chinese University of Hong Kong, Shatin, New Territories, Hong Kong, People's Republic of China

Received November 15, 2006

Icosahedral *o*-carboranes are readily reduced by group 1 metals to give "carbon atoms apart" (CAp) *nido*-carborane dianions that can be further reduced to the corresponding *arachno*-carborane tetraanions with the assistance of transition-metal ions. The geometries of the arachno species are dependent upon the electronic configurations of transition-metal ions. In contrast, "carbon atoms adjacent" (CAd) *nido*-carborane dianions can react with lithium metal, in the absence of any transition-metal ions, to produce CAd *arachno*-carborane tetraanions having a significantly different structure from their CAp counterparts. These CAd *nido*- and *arachno*-carborane anions possess a reducing power weaker than that of the CAp isomers, which can facilitate the capitation reactions of these anions with boron dihalides. This important discovery provides a very valuable entry point to the synthesis of 13- and 14-vertex carboranes. Subsequently, the largest heteroborane, 15-vertex metallacarborane, has been prepared. These studies open up new possibilities for the development of polyhedral clusters of extraordinary size. This review offers an overview of recent advances in this growing research field.

Introduction

Carboranes are derivatives of boron hydride clusters in which one or more BH vertices are substituted by CH. Of all known carboranes, the icosahedral *o*-$C_2B_{10}H_{12}$ (Chart 1) has been the most extensively investigated, owing to its commercial availability. Under strongly basic conditions, a formal $\{BH\}^{2+}$ vertex can be removed selectively from *o*-$C_2B_{10}H_{12}$ to form [*nido*-7,8-$C_2B_9H_{11}]^{2-}$ (named the dicarbollide ion, shown in Chart 1).[1] Recognition of the isolobal analogy between the cyclopentadienyl and dicarbollide ion initiated the field of metallacarborane chemistry.[2] This chemistry now appears in all modern textbooks dealing with inorganic and organometallic complexes. On the other hand, *o*-$C_2B_{10}H_{12}$ can be reduced by group 1 metals to give carbon atoms apart (CAp) [*nido*-7,9-$C_2B_{10}H_{12}]^{2-}$ (Chart 1), which is a very useful ligand for the production of 13-vertex metallacarboranes.[3,4] Efforts over almost half a century in this research field have resulted in extensive studies of the chemistry of [*nido*-7,8-$C_2B_9H_{11}]^{2-}$ and [*nido*-7,9-$C_2B_{10}H_{12}]^{2-}$ systems.[4] In sharp contrast, until 1999 the only known example of a metallacarborane containing an [*arachno*-$C_2B_{10}H_{12}]^{4-}$ ligand has been $(CpCo)_2(C_2B_{10}H_{12})$, prepared by two-electron reduction of $(\eta^5\text{-Cp})Co(\eta^6\text{-}C_2B_{10}H_{12})$ by Na, followed by addition of

Chart 1

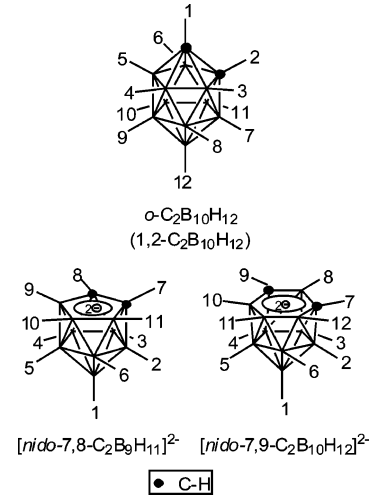

$CpNa/CoCl_2$ and air oxidation.[5a] A bicapped-hexagonal-antiprismatic geometry was proposed for this complex in 1974[5a] and was confirmed by single-crystal X-ray analyses in 2005.[5b,6] A question subsequently arises as to why the development of the coordination chemistry of [*arachno*-$R_2C_2B_{10}H_{10}]^{4-}$ anions is well behind that of [*nido*-$R_2C_2B_{10}H_{10}]^{2-}$. One may think of

* To whom correspondence should be addressed. E-mail: zxie@cuhk.edu.hk. Tel: +852 26096269. Fax: +852 26035057.

(1) (a) Wiesboeck, R. A.; Hawthorne, M. F. *J. Am. Chem. Soc.* **1964**, *86*, 1642. (b) Hawthorne, M. F.; Wegner, P. A.; Stafford, R. C. *Inorg. Chem.* **1965**, *4*, 1675.

(2) Hawthorne, M. F.; Young, D. C.; Wegner, P. A. *J. Am. Chem. Soc.* **1965**, *87*, 1818.

(3) (a) Fein, M.; Bobinski, J.; Mayes, N.; Schwartz, N.; Cohen, M. S. *Inorg. Chem.* **1963**, *2*, 1111. (b) Grafstein, D.; Dvorak, J. *Inorg. Chem.* **1963**, *2*, 1128. (c) Dunks, G. B.; Wiersema, R. J.; Hawthorne, M. F. *J. Am. Chem. Soc.* **1973**, *95*, 3174. (d) Tolpin, E. I.; Lipscomb, W. N. *Inorg. Chem.* **1973**, *12*, 2257. (e) Churchill, M. R.; DeBoer, B. G. *Inorg. Chem.* **1973**, *12*, 2674.

(4) (a) Grimes, R. N. Metallacarboranes. In *Comprehensive Organometallic Chemistry II*; Abel, E. W., Stone, F. G. A., Wilkinson, G., Eds.; Pergamon: New York, 1995; Vol. 1, pp 373. (b) Saxena, A. K.; Hosmane, N. S. *Chem. Rev.* **1993**, *93*, 1081. (c) Saxena, A. K.; Maguire, J. A.; Hosmane, N. S. *Chem. Rev.* **1997**, *97*, 2421. (d) Grimes, R. N. *Coord. Chem. Rev.* **2000**, *200/202*, 773. (e) Xie, Z. *Coord. Chem. Rev.* **2002**, *231*, 23. (f) Xie, Z. *Acc. Chem. Res.* **2003**, *36*, 1. (g) Xie, Z. *Coord. Chem. Rev.* **2006**, *250*, 259. (h) Corsini, M.; Fabrizi, de Biani, F.; Zanello. P. *Coord. Chem. Rev.* **2006**, *250*, 1351. (i) Kang, S. O.; Ko, J. *Adv. Organomet. Chem.* **2001**, *47*, 61.

10.1021/om061053d CCC: $37.00
Publication on Web 03/08/2007

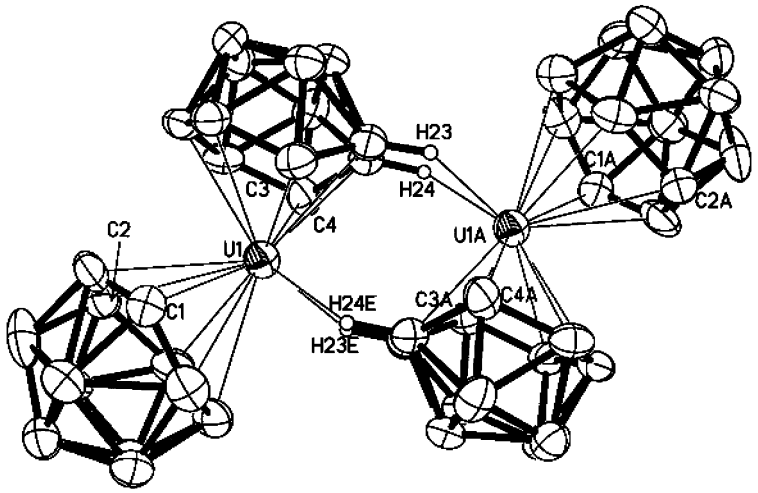

Figure 1. Structure of $[\{(\eta^7\text{-}C_2B_{10}H_{12})(\eta^6\text{-}C_2B_{10}H_{12})U\}_2]^{4-}$, reproduced by permission of Wiley-VCH from ref 7.

the following reasons: (1) the group 1 metal salts of [*arachno*-$R_2C_2B_{10}H_{10}]^{4-}$ are inaccessible, which are useful synthons for the preparation of metallacarboranes, (2) d-block transition metal ions are subject to reduction by group 1 metals during the reactions, and (3) significant rearrangement of the cage framework makes the reactions more complicated. In this connection, we wondered whether f-block elements are superior to d-block transition metals in the stabilization of *arachno*-carborane tetraanions, since f-block transition-metal ions are large and highly positive, yet stable to strong reducing agents, and they are not restricted to the 18-electron rule. We then initiated a research program in the late 1990s to explore the chemistry of the *arachno*-carborane system. This research has led to the discovery of a new bonding mode of [*arachno*-η^7-$R_2C_2B_{10}H_{10}]^{4-}$, the development of a methodology for the controlled synthesis of CAp and CAd (carbon atoms adjacent) *nido*- and *arachno*-carborane anions, and the first synthesis of a 14-vertex carborane and then a 15-vertex metallacarborane. This review attempts to provide an overview of such a research journey by highlighting our own work and the relevant studies from other groups.

It is noted that if no atom is indicated in the polyhedral structures shown in the following schemes, the vertex is a BH group. A black dot in the drawings represents a carbon atom. If a vertex contains an atom other than B and C, the heteroatom is shown explicitly.

CAp *arachno*-Carboranes of the C_2B_{10} System

The successful preparation of $(CpCo)_2(C_2B_{10}H_{12})$ suggests that the reduction of [*nido*-7,9-$R_2C_2B_{10}H_{10}]^{2-}$ to [*arachno*-$R_2C_2B_{10}H_{10}]^{4-}$ by group 1 metals can be achieved with the assistance of a transition-metal ion, although direct conversion from *o*-$R_2C_2B_{10}H_{10}$ to [*arachno*-$R_2C_2B_{10}H_{10}]^{4-}$ by group 1 metals is not feasible.[5] UCl_4 was initially chosen as the metal source for the production of [*arachno*-$C_2B_{10}H_{12}]^{4-}$, because uranium is an f element and its high oxidation state of +4 may match the [*arachno*-$C_2B_{10}H_{12}]^{4-}$ tetraanion. Interaction of *o*-$C_2B_{10}H_{12}$ with an excess of K metal in THF at room temperature followed by treatment with a suspension of UCl_4 in THF gave the uranacarborane $\{[(\eta^7\text{-}C_2B_{10}H_{12})(\eta^6\text{-}C_2B_{10}H_{12})U][K_2(THF)_5]\}_2$ in 58% yield (Scheme 1).[7] This complex represents not only the first metallacarborane containing an *arachno*-$[\eta^7\text{-}C_2B_{10}H_{12}]^{4-}$ ligand but also the first actinacarborane bearing an $[\eta^6\text{-}C_2B_{10}H_{12}]^{2-}$ ligand. Single-crystal X-ray analysis revealed that, in this centrosymmetric dimer, the [*nido*-$C_2B_{10}H_{12}]^{2-}$ and [*arachno*-$C_2B_{10}H_{12}]^{4-}$ ligands are bound to the U atom in η^6 and η^7 fashions, respectively, giving a bent-sandwich structural motif (Figure 1). The brand new η^7 bonding mode observed in this complex represents the highest hapticity for carboranyl ligands known to date. In this [η^7-*arachno*-$C_2B_{10}H_{12}]^{4-}$ anion, the five B atoms of the C_2B_5 bonding face are almost coplanar and the two C atoms are ~0.6 Å above this plane, engendering a boat-shaped geometry. As a result, the U−C(C_2B_5) bond distances are unexpectedly short, with an average value of 2.429(5) Å, which is comparable to those of known U−C σ bonds.[8] The average U−B(C_2B_5) distance of 2.780(6) Å is close to those found in other uranacarboranes.[9] The presence of the [*nido*-$C_2B_{10}H_{12}]^{2-}$ ligand in this complex is unexpected, as excess K metal does not reduce it to [*arachno*-$C_2B_{10}H_{12}]^{4-}$. Nonetheless, $[(\eta^7\text{-}C_2B_{10}H_{12})(\eta^6\text{-}C_2B_{10}H_{12})U]_2^{4-}$ could be viewed as an intermediate going from $[\eta^6\text{-}C_2B_{10}H_{12}]_2U$ to $\{[\eta^7\text{-}C_2B_{10}H_{12}]_2U\}^{4-}$.

Scheme 1

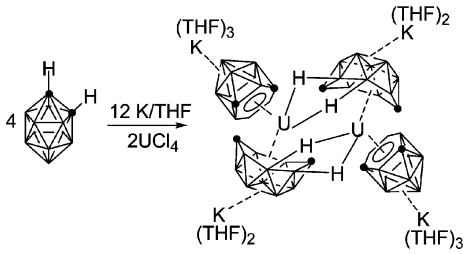

This result shows clearly that the geometry of the [*arachno*-$C_2B_{10}H_{12}]^{4-}$ ligand in $\{[(\eta^7\text{-}C_2B_{10}H_{12})(\eta^6\text{-}C_2B_{10}H_{12})U][K_2(THF)_5]\}_2$ is significantly different from that in $(CpCo)_2(C_2B_{10}H_{12})$,[5] which is probably related to the electronic configurations of the central metal ions. To examine the effect

(5) (a) Evans, W. J.; Hawthorne, M. F. *J. Chem. Soc., Chem. Commun.* **1974**, 38. (b) Ellis, D.; Lopez, M. E.; McIntosh, R.; Rosair, G. M.; Welch, A. J. *Chem. Commun.* **2005**, 1917.

(6) The geometry of the $M_2C_2B_{10}$ clusters is similar to that of the $M_2C_4B_8$ system; see: (a) Maxwell, W. M.; Bryan, R. F.; Sinn, E.; Grimes, R. N. *J. Am. Chem. Soc.* **1977**, *99*, 4008. (b) Maxwell, W. M.; Bryan, R. F.; Sinn, E.; Grimes, R. N. *J. Am. Chem. Soc.* **1977**, *99*, 4016. (c) Pipal, J. R.; Grimes, R. N. *Inorg. Chem.* **1978**, *17*, 6.

(7) Xie, Z.; Yan. C.; Yang, Q.; Mak, T. C. W. *Angew. Chem., Int. Ed.* **1999**, *38*, 1761.

(8) (a) Perego, G.; Asari, M.; Farina, F.; Lugli, G. *Acta Crystallogr., Sect. B* **1976**, *32*, 3034. (b) Arnaudet, L.; Charpin, P.; Folcher, G.; Lance, M.; Nierlich, M.; Vigner, D. *Organometallics* **1986**, *5*, 270. (c) Halstead, G. W.; Baker, E. C.; Raymond, K. N. *J. Am. Chem. Soc.* **1975**, *97*, 3049.

(9) (a) Fronczek, F. R.; Halstead, G. W.; Raymond, K. N. *J. Am. Chem. Soc.* **1977**, *99*, 1769. (b) Rabinovich, D.; Haswell, C. M.; Scott, B. L.; Miller, R. L.; Nielsen, J. B.; Abney, K. D. *Inorg. Chem.* **1996**, *35*, 1425.

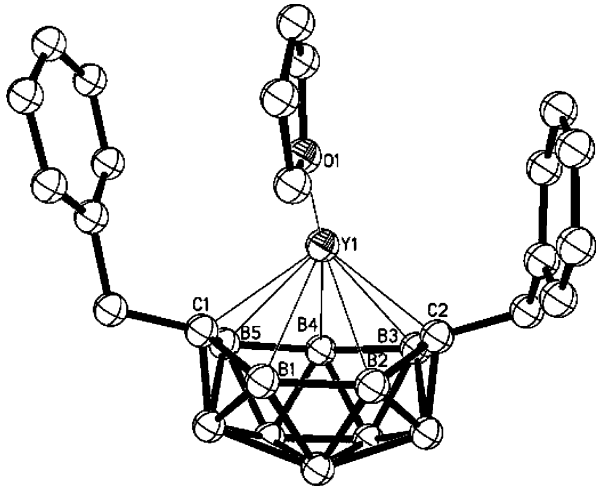

Figure 2. Structure of $[\{\eta^7\text{-}(C_6H_5CH_2)_2C_2B_{10}H_{10}\}Y(THF)]^-$, reproduced by permission of the American Chemical Society from ref 10.

Scheme 2

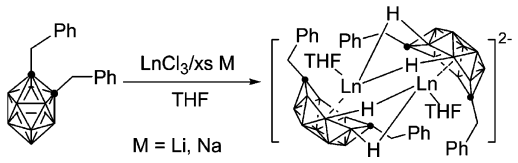

of the central metal ions, the lanthanides were chosen to replace uranium in the above reaction. Treatment of 1,2-$(C_6H_5CH_2)_2$-1,2-$C_2B_{10}H_{10}$ with an excess of Na or Li metal in THF in the presence of lanthanide trichlorides gave the 13-vertex lanthanacarboranes $\{[\eta^7\text{-}(C_6H_5CH_2)_2C_2B_{10}H_{10}]M(THF)\}_2\{Na(THF)_3\}_2$ or $[\{\eta^7\text{-}(C_6H_5CH_2)_2C_2B_{10}H_{10}\}M(THF)]_2[Li(THF)_4]_2$ (M = Y, Dy, Er) in moderate to good yields, respectively (Scheme 2).[10] Single-crystal X-ray diffraction studies revealed that, like the [*arachno*-$C_2B_{10}H_{12}]^{4-}$ ligand in the aforementioned uranacarborane, the [*arachno*-$(C_6H_5CH_2)_2C_2B_{10}H_{10}]^{4-}$ in these lanthanacarboranes is also bonded to the M^{3+} ion in an η^7 fashion.[10] Figure 2 shows the representative bonding interactions between [*arachno*-$(C_6H_5CH_2)_2C_2B_{10}H_{10}]^{4-}$ and Y^{3+}. Such a unique cage arrangement leads to three different types of coordination environments for the cage atoms: five-coordinate carbon, six-coordinate boron, and seven-coordinate boron, respectively. The cage carbon atoms are unambiguously identified by the attached benzyl groups. The M−C(cage) distances are at the short end of the range for M−C σ bonds.[11] Since the reduction of 1,2-$(C_6H_5CH_2)_2$-1,2-$C_2B_{10}H_{10}$ with an excess of group 1 metals does not give an arachno species but rather affords [*nido*-7,9-$(C_6H_5CH_2)_2$-7,9-$C_2B_{10}H_{10}]^{2-}$,[12] it is reasonable to suggest that the lanthanacarboranes $[\eta^6\text{-}(C_6H_5CH_2)_2C_2B_{10}H_{10}]MCl(THF)_x$ may serve as the intermediates which accept two more electrons from Na metal to form the final products.

To test this hypothesis, the 13-vertex erbacarborane $[\eta^5{:}\eta^6\text{-}Me_2C(C_5H_4)(C_2B_{10}H_{11})]Er(THF)_2$, bearing a CAp *nido*-carborane ligand, was prepared and subsequently used as a starting material.[13] Indeed, it reacted with an excess of Na metal in THF to generate the new 13-vertex species $[\{[\eta^5{:}\eta^7\text{-}Me_2C(C_5H_4)(C_2B_{10}H_{11})]Er\}_2\{Na_4(THF)_9\}]_n$, having an *arachno*-carborane

Scheme 3

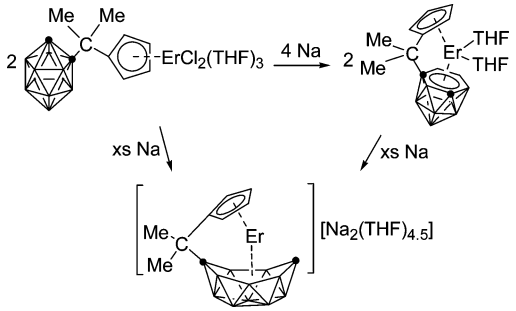

ligand (Scheme 3), whose structure was confirmed by single-crystal X-ray analyses.[13] This complex was, on the other hand, also synthesized by the direct interaction of $[\eta^5\text{-}Me_2C(C_5H_4)(C_2B_{10}H_{11})]ErCl_2(THF)_3$ with an excess of sodium metal (Scheme 3).[13] These results strongly support the reaction pathway suggested above. Under similar reaction conditions, other substituted carboranes such as $Me_2Si(C_9H_7)(C_2B_{10}H_{11})$, $Me_2Si(C_{13}H_9)(C_2B_{10}H_{11})$, $(ArCH_2)_2C_2B_{10}H_{10}$ (Ar = 3,5-$(CH_3O)_2C_6H_3$, 1-pyrenyl), $(XCH_2CH_2)C_2B_{10}H_{11}$, $(XCH_2CH_2)_2C_2B_{10}H_{10}$, $(XCH_2CH_2)(X'CH_2CH_2)C_2B_{10}H_{10}$ (X, X′ = MeO, Me_2N), and $(C_9H_7)C_2B_{10}H_{11}$ can all be converted to the corresponding *arachno*-η^7-carboranyl ligands without exception.[14−16] Reactivity studies on the complex $[\{\eta^1{:}\eta^7\text{-}[(Me_2NCH_2CH_2)C_2B_{10}H_{11}]Er(THF)\}\{Na(THF)_3\}]_2$ indicated that the $\{\eta^1{:}\eta^7\text{-}[(Me_2NCH_2CH_2)C_2B_{10}H_{11}]Er\}^-$ moiety remains intact, although the associated complex cation $\{Na(THF)_3\}^+$ can be substituted by other cations such as $\{K(18\text{-crown-6})\}^+$ and $\{Mg(NCMe)_6\}^{2+}$. This complex shows no reactivity toward unsaturated molecules: for example, PhNCO, ^{t}BuNC, and 2,6-Me_2-C_6H_3NC.[16a]

The above results show that (1) the geometry of *arachno*-$[\eta^7\text{-}R_2C_2B_{10}H_{10}]^{4-}$ is the same, regardless of substituents on the cage carbons and f elements, and (2) *arachno*-$[\eta^7\text{-}R_2C_2B_{10}H_{10}]^{4-}$ prefers metal ions with d^0/f^n electronic configurations. These characteristics can be explained via DFT calculations on the model complex $[(\eta^7\text{-}C_2B_{10}H_{12})Y(H_2O)]_2^{2-}$. Careful examination of the molecular orbitals indicates that the five d orbitals of Y are all significantly involved in the metal−$[\eta^7\text{-}C_2B_{10}H_{12}]$ bonding interactions. The relevant molecular orbitals are mainly found in the HOMO−LUMO region. A schematic molecular orbital interaction diagram is shown in Figure 3.[10] The *arachno*-$[\eta^7\text{-}C_2B_{10}H_{12}]^{4-}$ moiety contributes five pairs of electrons to the five bonding orbitals. Any d electrons of the central metal ion will go to the antibonding orbitals, which destabilizes the M−$[\eta^7\text{-}C_2B_{10}H_{12}]$ bonding interaction and leads to the rearrangement from $[\eta^7\text{-}C_2B_{10}H_{12}]^{4-}$ to $[\eta^6{:}\eta^6\text{-}C_2B_{10}H_{12}]^{4-}$ to meet the requirements of the 18-electron rule. These calculations further suggest that the *arachno*-η^7-carboranyl ligand should be able to stabilize the metal ions in their highest oxidation state, and only f-elements can form full-sandwich metallacarboranes with η^7-carboranyl ligands.

These predictions have proved to be correct through the isolation of the high-valent metallacarboranes $\{\{[\eta^7\text{-}Me_2Si(C_{13}H_9)(C_2B_{10}H_{11})]_2Yb\}_2Yb\}\{Na_8(THF)_{20}\}$,[14a] $[\{(\mu\text{-}\eta^5){:}\eta^7\text{-}Me_2$-

(10) Chui, K.; Yang, Q.; Mak, T. C. W.; Lam, W.-H.; Lin, Z.; Xie, Z. *J. Am. Chem. Soc.* **2000**, *122*, 5758.
(11) Cotton, S. A. *Coord. Chem. Rev.* **1997**, *160*, 93.
(12) Chui, K.; Li, H.-W.; Xie, Z. *Organometallics* **2000**, *19*, 5447.
(13) Xie, Z.; Chui, K.; Yang, Q.; Mak, T. C. W. *Organometallics* **1999**, *18*, 3947.
(14) (a) Wang, S.; Li, H.-W.; Xie, Z. *Organometallics* **2001**, *20*, 3842. (b) Wang, S.; Wang, Y.; Cheung, M.-S.; Chan, H.-S.; Xie, Z. *Tetrahedron* **2003**, *59*, 10373.
(15) Shen, H.; Chan, H.-S.; Xie, Z. *Organometallics* **2006**, *25*, 2617.
(16) (a) Cheung, M.-S.; Chan, H.-S.; Xie, Z. *Organometallics* **2005**, *24*, 4468. (b) Cheung, M.-S.; Chan, H.-S.; Xie, Z. *Organometallics* **2004**, *23*, 517.

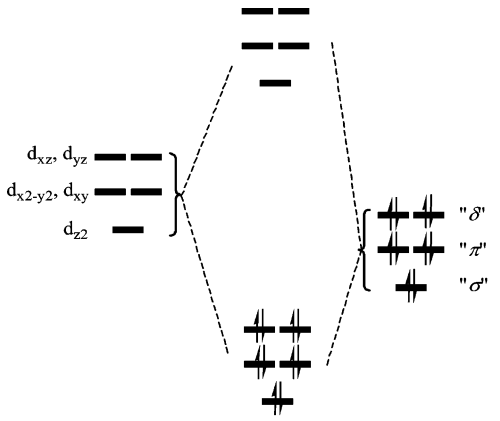

Figure 3. Schematic orbital interaction diagram of Y^{3+} with $[arachno\text{-}\eta^7\text{-}C_2B_{10}H_{12}]^{4-}$, reproduced by permission of the American Chemical Society from ref 10.

Scheme 4

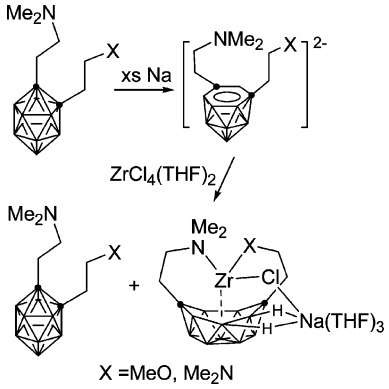

$Si(C_5H_4)(C_2B_{10}H_{11})\}Zr(NEt_2)_2\{Na_3(THF)_4\}]_n$,[17] $[\eta^1{:}\eta^1{:}\eta^7\text{-}(Me_2NCH_2CH_2)_2(C_2B_{10}H_{10})]Zr(\mu\text{-}Cl)Na(THF)_3$,[18] $[\eta^1{:}\eta^1{:}\eta^7\text{-}(Me_2NCH_2CH_2)(MeOCH_2CH_2)(C_2B_{10}H_{10})]Zr(\mu\text{-}Cl)Na(THF)_3$,[18] and $[\{\eta^1{:}\eta^7\text{-}[(Me_2NCH_2CH_2)(C_2B_{10}H_{11})]Sm(THF)\}_4Sm][Na(THF)_4]$[18] in the presence of an excess of Na metal in THF. It is noteworthy that the last three complexes were prepared via an unexpected functional side-arm-promoted electron-transfer reaction, which provides a new method for the synthesis of metallacarboranes incorporating $[\eta^7\text{-}R_2C_2B_{10}H_{10}]^{4-}$ ligands.[18] Treatment of $[7\text{-}(Me_2NCH_2CH_2)\text{-}9\text{-}(XCH_2CH_2)\text{-}7,9\text{-}C_2B_{10}H_{10}][Na_2(THF)_x]$ with 1 equiv of $ZrCl_4(THF)_2$ in THF gave the high-valent zirconacarboranes $[\eta^1{:}\eta^1{:}\eta^7\text{-}(Me_2NCH_2CH_2)(XCH_2CH_2)(C_2B_{10}H_{10})]Zr(\mu\text{-}Cl)Na(THF)_3$ and $1\text{-}Me_2NCH_2CH_2\text{-}2\text{-}XCH_2CH_2\text{-}1,2\text{-}C_2B_{10}H_{10}$ in a 1:1 molar ratio (X = MeO, Me_2N) (Scheme 4).[18] Figure 4 shows the molecular structure of $[\eta^1{:}\eta^1{:}\eta^7\text{-}(Me_2NCH_2CH_2)(Me_2NCH_2CH_2)(C_2B_{10}H_{10})]Zr(\mu\text{-}Cl)Na(THF)_3$. The formation of the Zr(IV) complexes is unprecedented, as the known reactions of $[nido\text{-}7,9\text{-}R_2\text{-}7,9\text{-}C_2B_{10}H_{10}]^{2-}$ with $ZrCl_4$ usually gave the Zr(II) complex $[(\eta^6\text{-}R_2C_2B_{10}H_{10})_2Zr]^{2-}$ due to the strong reducing power of the *nido*-carborane dianions.[19] Theoretical studies revealed that the functional side arm is both electronically and entropically necessary for electron transfer from the Zr(II) metal center, formed by the redox reaction between $ZrCl_4$ and $[(Me_2NCH_2CH_2)(XCH_2CH_2)(C_2B_{10}H_{10})]^{2-}$, to the *nido*-carborane cage, leading to the formation of the final product.[18] The isolation of the Sm(III) complex $[\{\eta^1{:}\eta^7\text{-}[(Me_2NCH_2CH_2)(C_2B_{10}H_{11})]Sm(THF)\}_4Sm][Na(THF)_4]$ from the reaction of $[7\text{-}(Me_2NCH_2CH_2)\text{-}7,9\text{-}C_2B_{10}H_{11}]Na_2$ with SmI_2 supports this reaction pathway (Scheme 5).[18] Accordingly, controlled synthesis of CAp divalent metallacarboranes of the types $[(nido\text{-}R_2C_2B_{10}H_{10})_2M]^{2-}$ (M = group 4 metals)[19] and $(nido\text{-}R_2C_2B_{10}H_{10})Ln$ (Ln = Sm, Eu, Yb)[20] or high-valent metallacarboranes of the types $(arachno\text{-}R_2C_2B_{10}H_{10})M$[17,18] and $(arachno\text{-}R_2C_2B_{10}H_{10})Ln^-$ [10,12−18] can be achieved by changing the nature of the substituents R.

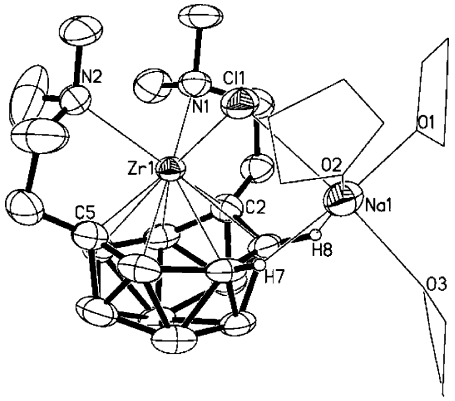

Figure 4. Structure of $[\eta^1{:}\eta^1{:}\eta^7\text{-}(Me_2NCH_2CH_2)(Me_2NCH_2CH_2)(C_2B_{10}H_{10})]Zr(\mu\text{-}Cl)Na(THF)_3$, reproduced by permission of the American Chemical Society from ref 18.

Scheme 5

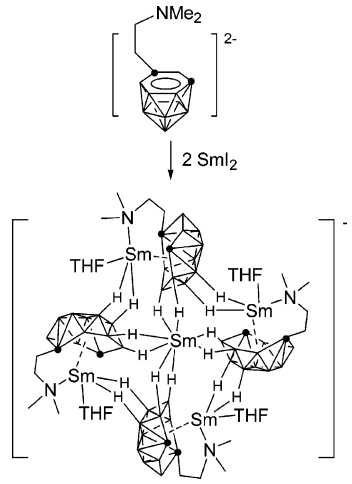

CAd *nido*- and *arachno*-Carboranes of the C_2B_{10} System

It is well-documented that $o\text{-}R_2C_2B_{10}H_{10}$ can be readily reduced by group 1 metals to give CAp $[7,9\text{-}R_2C_2B_{10}H_{10}]M_2$ (M = group 1 metals), which are useful synthons for the production of 13-vertex metallacarboranes.[3,4] Their structures, however, remained unknown until 2000, after the first structural characterization of $[(C_6H_5CH_2)_2C_2B_{10}H_{10}]Na_2(THF)_4$.[12] These

(17) Wang, Y.; Wang, H.; Li, H.-W.; Xie, Z. *Organometallics* **2002**, *21*, 3311.

(18) Cheung, M.-S.; Chan, H.-S.; Bi, S.; Lin, Z.; Xie, Z. *Organometallics* **2005**, *24*, 4333.

(19) (a) Salentine, C. G.; Hawthorne, M. F. *J. Am. Chem. Soc.* **1975**, *97*, 426. (b) Lo, F. Y.; Strouse, C. E.; Callahan, K. P.; Knobler, C. B.; Hawthorne, M. F. *J. Am. Chem. Soc.* **1975**, *97*, 428. (c) Salentine, C. G.; Hawthorne, M. F. *Inorg. Chem.* **1976**, *15*, 2872.

(20) (a) Khattar, R.; Knobler, C. B.; Johnson, S. E.; Hawthorne, M. F. *Inorg. Chem.* **1991**, *30*, 1972. (b) Khattar, R.; Manning, M. J.; Knobler, C. B.; Johnson, S. E.; Hawthorne, M. F. *Inorg. Chem.* **1992**, *31*, 268. (c) Xie, Z.; Wang, S.; Zhou, Z.-Y.; Mak, T. C. W. *Organometallics* **1999**, *18*, 1641. (d) Xie, Z.; Liu, Z.; Yang, Q.; Mak, T. C. W. *Organometallics* **1999**, *18*, 3603.

Scheme 6

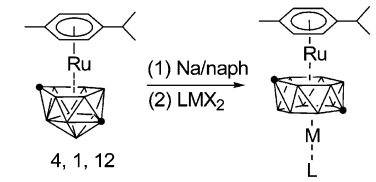

LM = CpCo, (dppe)Ni, (p-cymene)Ru, (C_6H_6)Ru

Scheme 7

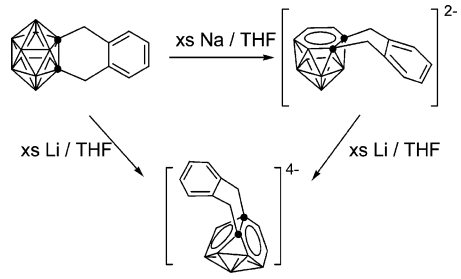

results clearly show that the reduction of *o*-carboranes always leads to the separation of two cage carbon vertices, forming CAp *nido*-carboranes. We wondered whether the relative positions of cage carbon vertices could be controlled during the reductive process. The most effective way to achieve this goal probably is to introduce a suitable linkage between the two cage carbon atoms.

Reduction of μ-1,2-[*o*-$C_6H_4(CH_2)_2$]-1,2-$C_2B_{10}H_{10}$ with an excess of Na metal in THF afforded the CAd *nido*-carborane salt [{μ-7,8-[*o*-$C_6H_4(CH_2)_2$]-7,8-$C_2B_{10}H_{10}$}$_2$Na$_4$(THF)$_6$]$_n$ in high yield (Scheme 7).[21] X-ray diffraction studies showed that the *nido*-carborane anion {μ-7,8-[*o*-$C_6H_4(CH_2)_2$]-7,8-$C_2B_{10}H_{10}$}$^{2-}$ has an open six-membered C_2B_4 face in which the two cage carbon atoms remain in adjacent positions with a bond distance of 1.444(4) Å. The six cage atoms of this C_2B_4 open face are nearly coplanar and are bonded to a sodium atom in η^6 fashion with an average distance of 2.854(4) Å, which is comparable to that found in CAp [$(C_6H_5CH_2)_2C_2B_{10}H_{10}$]Na$_2(THF)_4$.[12] Figure 5 shows the structure of CAd {μ-7,8-[*o*-$C_6H_4(CH_2)_2$]-7,8-$C_2B_{10}H_{10}$}$^{2-}$. In a similar manner, the full-sandwich potassacarborane [{μ-7,8-[*o*-$C_6H_4(CH_2)_2$]-7,8-$C_2B_{10}H_{10}$}$_2$K$_3$(18-crown-6)$_2$][(18-crown-6)K(CH$_3$CN)$_2$], bearing the same CAd carboranyl ligand, also was obtained.[22]

Interestingly, this CAd *nido*-carborane dianion shows a redox property different from that of its CAp counterparts, as it can be further reduced by Li metal to give the CAd *arachno* salt [{μ-1,2-[*o*-$C_6H_4(CH_2)_2$]-1,2-$C_2B_{10}H_{10}$}Li$_4$(THF)$_6$]$_2$ without the assistance of any transition-metal ions (Scheme 7).[21] This arachno salt can also be directly prepared by reduction of μ-1,2-[*o*-$C_6H_4(CH_2)_2$]-1,2-$C_2B_{10}H_{10}$ with an excess of Li metal (Scheme 7).[21] It represents the first group 1 metal salt of *arachno*-[$R_2C_2B_{10}H_{10}$]$^{4-}$. Single-crystal X-ray analyses revealed that the cage geometry of this arachno species is significantly different from those of the CAp species *arachno*-[η^7-R_2-$C_2B_{10}H_{10}$]$^{4-}$ and *arachno*-[η^6:η^6-$C_2B_{10}H_{12}$]$^{4-}$ (Scheme 6).[5−7] As shown in Figure 6, the tetraanion {μ-1,2-[*o*-$C_6H_4(CH_2)_2$]-1,2-$C_2B_{10}H_{10}$}$^{4-}$ consists of one open six-membered C_2B_4 face and one open five-membered C_2B_3 face that are bonded to two lithium atoms in η^6 and η^5 fashions, respectively. These two open faces share one common edge of a C(cage)−C(cage) bond with a distance of 1.564(3) Å. Careful examination of the

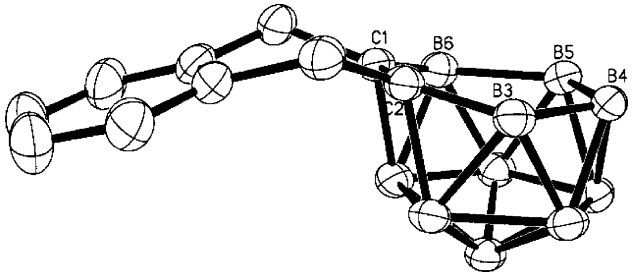

Figure 5. Structure of {μ-7,8-[*o*-$C_6H_4(CH_2)_2$]-7,8-$C_2B_{10}H_{10}$}$^{2-}$, reproduced by permission of the American Chemical Society from ref 21.

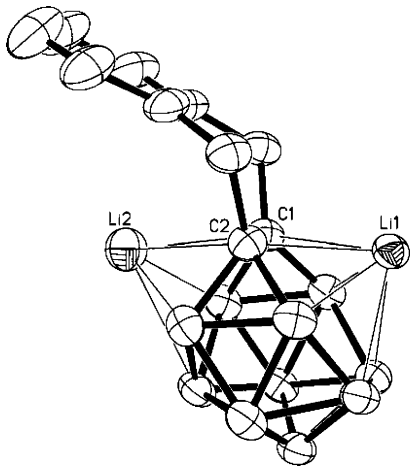

Figure 6. Interaction of {μ-1,2-[*o*-$C_6H_4(CH_2)_2$]-1,2-$C_2B_{10}H_{10}$}$^{4-}$ with Li^+ cations, reproduced by permission of the American Chemical Society from ref 21.

Chart 2

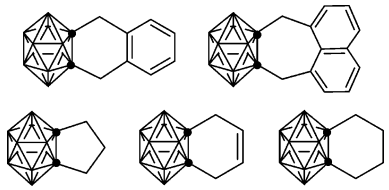

molecular structures of the nido and arachno anions indicates that the bent five-membered face is generated by breaking a B−B connectivity of the *nido*-carborane via two-electron uptake from lithium. It is worth noting that Na and K metals cannot directly reduce μ-1,2-[*o*-$C_6H_4(CH_2)_2$]-1,2-$C_2B_{10}H_{10}$ to the corresponding arachno species. Following this motif, a new class of CAd *nido*- and *arachno*-carborane anions has been prepared via a reduction of C,C′-linked *o*-carboranes with group 1 metals (Chart 2). Exam-ples include [{μ-7,8-[1′,8′-$C_{10}H_6(CH_2)_2$]-7,8-$C_2B_{10}H_{10}$}$_2$Na$_4$(THF)$_6$]$_n$, [{μ-7,8-$(CH_2)_3$-7,8-$C_2B_{10}H_{10}$}Na$_2$(THF)$_4$]$_n$, [{μ-1,2-[1′,8′-$C_{10}H_6(CH_2)_2$]-1,2-$C_2B_{10}H_{10}$}Li$_4$(THF)$_6$]$_2$, [{μ-1,2-$(CH_2)_3$-1,2-$C_2B_{10}H_{10}$}{Li$_4$(THF)$_5$}]$_2$, [{μ-1,2-(CH$_2$CH═CHCH$_2$)-1,2-C_2B_{10}-H$_{10}$}{Li$_4$(THF)$_5$}]$_2$, and [{μ-1,2-$(CH_2)_4$-1,2-$C_2B_{10}H_{10}$}{Li$_4$-(THF)$_5$}]$_2$.[23,24]

The length and rigidity of the bridge between the two cage carbon atoms have large effects on the relative positions of the cage carbon atoms of the final products. Treatment of μ-1,2-$(CH_2)_5$-1,2-$C_2B_{10}H_{10}$, μ-1,2-[1′,1″-$(C_6H_4)_2$-2′,2″-$(CH_2)_2$]-1,2-$C_2B_{10}H_{10}$, and μ-1,2-$(CH_2)_6$-1,2-$C_2B_{10}H_{10}$ with an excess of Li or Na metal in THF afforded the CAp *nido*-carborane anions

(21) Zi, G.; Li, H.-W.; Xie, Z. *Organometallics* **2001**, *20*, 3836.
(22) Zi, G.; Li, H.-W., Xie, Z. *Chem. Commun.* **2001**, 1110.
(23) Zi, G.; Li, H.-W.; Xie, Z. *Organometallics* **2002**, *21*, 5415.
(24) Deng, L.; Cheung, M.-S.; Chan, H.-S.; Xie, Z. *Organometallics* **2005**, *24*, 6244.

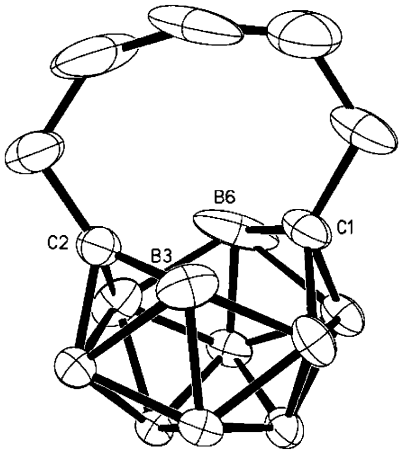

Figure 7. Structure of $[\mu\text{-}7,10\text{-}(CH_2)_5\text{-}7,10\text{-}C_2B_{10}H_{10}]^{2-}$, reproduced by permission of the American Chemical Society from ref 24.

Scheme 8

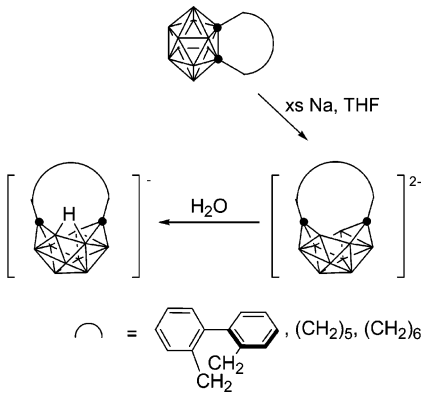

$[\mu\text{-}7,10\text{-}(CH_2)_5\text{-}7,10\text{-}C_2B_{10}H_{10}]^{2-}$, $\{\mu\text{-}7,10\text{-}[1',1''\text{-}(C_6H_4)_2\text{-}2',2''\text{-}(CH_2)_2]\text{-}7,10\text{-}C_2B_{10}H_{10}\}^{2-}$, and $[\mu\text{-}7,10\text{-}(CH_2)_6\text{-}7,10\text{-}C_2B_{10}H_{10}]^{2-}$, respectively (Scheme 8).[23,24] No *arachno*-carborane species were detected by ^{11}B NMR techniques. X-ray analyses showed that these CAp $[nido\text{-}7,10\text{-}R_2C_2B_{10}H_{10}]^{2-}$ dianions have a basket geometry with a highly distorted six-membered C_2B_4 open face. Structural comparisons between the *nido*-carborane anions and their parent *closo*-carboranes indicate that the reduction process disrupts partially the closo cage by breaking the C(1)···C(2), C(1)···B(3), and C(2)···B(6) connectivities. The longer the linkage is, the greater the C(cage)···C(cage) separation will be, as evidenced by its distance ranging from 2.687(6) to 2.836(4) to 2.872(7) Å, observed in the aforementioned CAp *nido*-carborane anions. Figure 7 shows the structure of $[\mu\text{-}7,10\text{-}(CH_2)_5\text{-}7,10\text{-}C_2B_{10}H_{10}]^{2-}$.[24]

These results show that although both the length and rigidity of the bridges in C,C′-linked *o*-carboranes have significant effects on the formation of carborane anions, the former plays a more important role than the latter in controlling the relative positions of the two cage carbon atoms during the reductive process. If there are six bridging carbon atoms, the cage carbon−carbon bond is completely broken during two-electron reduction to generate CAp *nido*-carborane dianions, regardless of the nature of the bridges. When there are five bridging carbon atoms, the rigidity of the bridge dominates the relative positions of the cage carbon atoms during the reduction process. A more rigid five-carbon-atom bridge locks the two cage carbon atoms in ortho positions, offering CAd carborane anions. On the other hand, a less rigid bridge allows the two cage carbon atoms to move apart, generating CAp *nido*-carborane dianions. This also

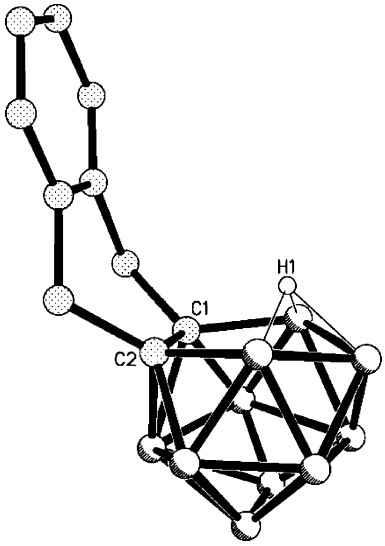

Figure 8. Structure of $\{\mu\text{-}8,9\text{-}[o\text{-}C_6H_4(CH_2)_2]\text{-}8,9\text{-}C_2B_{10}H_{11}\}^{-}$, reproduced by permission of the American Chemical Society from ref 23 (other terminal H atoms are omitted for clarity).

Scheme 9

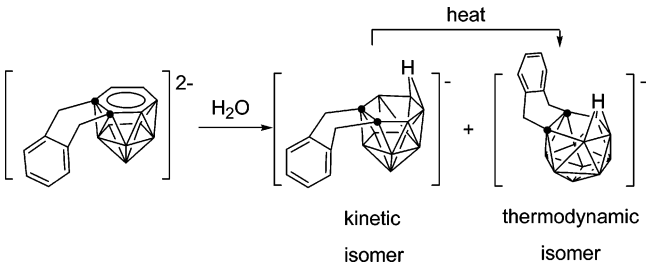

indicates clearly that only CAd *nido*-carboranes can be further reduced by Li metal to produce the corresponding CAd *arachno*-carboranes. It strongly suggests that CAd *nido*-carboranes are weaker reducing agents than CAp nido species or that CAd *nido*-carboranes have a stronger oxidizing power than the CAp nido counterparts, as the latter show no reactivity toward Li metal.

All CAd *nido*- and *arachno*-carborane anions are very air- and moisture-sensitive. They can be readily oxidized by oxidants such as O_2 back to neutral *o*-carboranes.[23,24] Hydrolysis converts both *nido*- and *arachno*-carborane anions to the corresponding carborane monoanions by one- and three-proton uptake from water, respectively.[23] For example, reaction of $\{\mu\text{-}7,8\text{-}[o\text{-}C_6H_4\text{-}(CH_2)_2]\text{-}7,8\text{-}C_2B_{10}H_{10}\}^{2-}$ with degassed water in THF at room temperature generated the monoanion $\{\mu\text{-}7,8\text{-}[o\text{-}C_6H_4(CH_2)_2]\text{-}\mu\text{-}10,11\text{-H-}7,8\text{-}C_2B_{10}H_{10}\}^{-}$, which can be converted to its thermodynamically more stable isomer $\{\mu\text{-}8,9\text{-}[o\text{-}C_6H_4(CH_2)_2]\text{-}\mu\text{-}10,11,12\text{-H-}8,9\text{-}C_2B_{10}H_{10}\}^{-}$ upon heating (Scheme 9).[23] This conversion is quite different from that of the CAp *nido*-$[7,9\text{-}R_2C_2B_{10}H_{10}]^{2-}$ system, in which the carbon extrusion species is the thermodynamic product.[12,25] Figure 8 shows the structure of this thermodynamically stable anion $\{\mu\text{-}8,9\text{-}[o\text{-}C_6H_4(CH_2)_2]\text{-}8,9\text{-}C_2B_{10}H_{11}\}^{-}$. It is noted that the protonation of $[nido\text{-}7,10\text{-}R_2C_2B_{10}H_{10}]^{2-}$ with degassed water in the temperature range 0−60 °C only gave one isomer, probably due to its constrained geometry (Scheme 8).[23] This isomer was proposed to be $[\mu\text{-}8,9\text{-H-}7,10\text{-}R_2C_2B_{10}H_{10}]^{-}$, according to the spectroscopic data. Protonation of $\{\mu\text{-}1,2\text{-}[o\text{-}C_6H_4(CH_2)_2]\text{-}1,2\text{-}C_2B_{10}H_{10}\}^{4-}$ afforded a thermodynamic isomer upon heating, $[\mu\text{-}1,2\text{-}[o\text{-}C_6H_4(CH_2)_2]\text{-}$

(25) (a) Getman, T. G.; Knobler, C. B.; Hawthorne, M. F. *Inorg. Chem.* **1990**, *29*, 158. (b) Tolpin, E. I.; Lipscomb, W. N. *Inorg. Chem.* **1973**, *12*, 2257. (c) Churchill, M. R.; DeBoer, B. G. *Inorg. Chem.* **1973**, *12*, 2674.

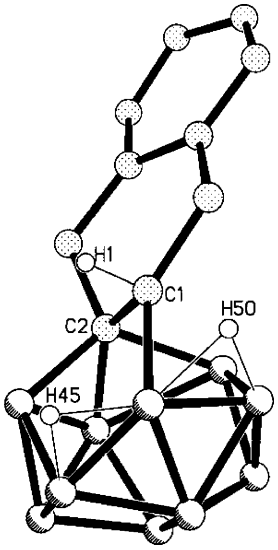

Figure 9. Structure of $[\mu$-1,2-[o-$C_6H_4(CH_2)_2$]-1,2-$C_2B_{10}H_{13}]^-$, reproduced by permission of the American Chemical Society from ref 23 (other terminal H atoms are omitted for clarity).

Scheme 10

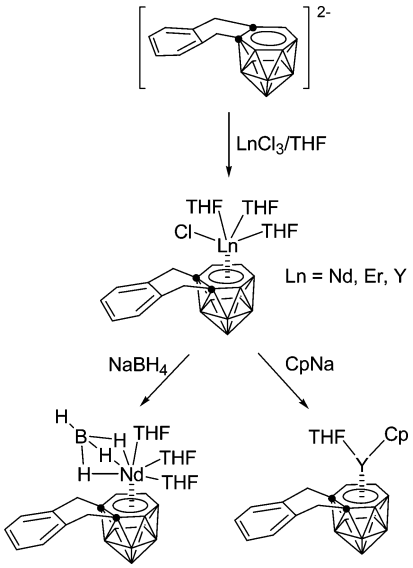

$1,2\text{-}C_2B_{10}H_{13}]^-$. Single-crystal X-ray analyses revealed that its structure is distinct from that of the parent *arachno*-carborane anion $\{\mu$-1,2-[*o*-$C_6H_4(CH_2)_2$]-1,2-$C_2B_{10}H_{10}\}^{4-}$, as shown in Figure 9.[23]

Group 1 metal salts of both CAd *nido*- and *arachno*-carborane anions are useful synthons for the preparation of a new class of CAd metallacarboranes. Treatment of CAd $[\{\mu$-7,8-[*o*-C_6H_4-$(CH_2)_2$]-7,8-$C_2B_{10}H_{10}\}_2Na_4(THF)_6]_n$ with 2 equiv of $LnCl_3$ in THF generated the half-sandwich 13-vertex lanthanacarborane chlorides 4-Cl-4,4,4-$(THF)_3$-μ-1,2-[*o*-$C_6H_4(CH_2)_2$]-4,1,2-LnC_2-$B_{10}H_{10}$ (Ln = Nd, Er, Y) (Scheme 10).[26] The monomeric structure of the erbium complex has been confirmed by an X-ray diffraction study. As shown in Figure 10, the Er atom is η^6 bound to a hexagonal bonding face of the CAd carboranyl, σ-bound to a terminal chloro ligand, and coordinated to three THF molecules in a distorted-square-pyramidal geometry. The terminal Er−Cl distance of 2.542(4) Å is comparable to those normally observed in organoerbium chloride complexes.[27] The average Er−cage atom distance of 2.77(2) Å is comparable to

(26) Zi, G.; Li, H.-W.; Xie, Z. *Organometallics* **2002**, *21*, 3464.

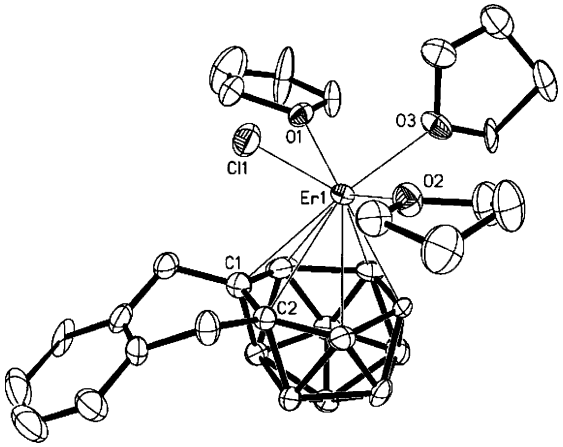

Figure 10. Structure of 4-Cl-4,4,4-$(THF)_3$-μ-1,2-[*o*-$C_6H_4(CH_2)_2$]-4,1,2-$ErC_2B_{10}H_{10}$, reproduced by permission of the American Chemical Society from ref 26.

Scheme 11

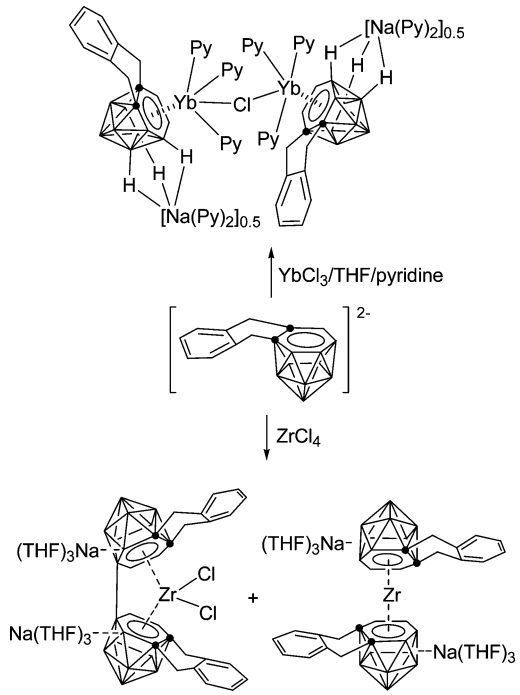

that of 2.705(7) Å found in $[\eta^5{:}\eta^6$-$Me_2C(C_5H_4)(C_2B_{10}H_{11})]Er$-$(THF)_2$.[13] The chloro group in these complexes can be substituted by other moieties, leading to the isolation of 4-$[(\mu$-H$)_3$BH]-4,4,4-$(THF)_3$-μ-1,2-[*o*-$C_6H_4(CH_2)_2$]-4,1,2-$NdC_2B_{10}H_{10}$ and 4-(η^5-C_5H_5)-4-THF-μ-1,2-[*o*-$C_6H_4(CH_2)_2$]-4,1,2-$YC_2B_{10}H_{10}$ (Scheme 10).[26]

Although the reducing power of CAd *nido*-carborane dianions is weaker than that of the CAp counterparts, as discussed previously, they can still reduce high-valent metal ions to their lower oxidation states. Reaction of $[\{\mu$-7,8-[*o*-$C_6H_4(CH_2)_2$]-7,8-$C_2B_{10}H_{10}\}_2Na_4(THF)_6]_n$ with 2 equiv of $YbCl_3$ gave the Yb(II) complex $\{4,4,4\text{-}(NC_5H_5)_3\text{-}4\text{-}(\mu\text{-}Cl)_{0.5}\text{-}\mu\text{-}1,2\text{-}[o\text{-}C_6H_4(CH_2)_2]\text{-}4,1,2\text{-}YbC_2B_{10}H_{10}\}_2\{Na(NC_5H_5)_2\}$ (Scheme 11).[26] Treatment of $[\{\mu$-7,8-[*o*-$C_6H_4(CH_2)_2$]-7,8-$C_2B_{10}H_{10}\}_2Na_4(THF)_6]_n$ with $ZrCl_4$ in THF yielded the Zr(II) species $\{[o\text{-}C_6H_4(CH_2)_2C_2B_{10}H_{10}]_2\text{-}Zr\}\{Na(THF)_3\}_2$ as the major product and the Zr(IV) complex

(27) For reviews, see: (a) Schumann, H.; Messe-Markscheffel, J. A.; Esser, L. *Chem. Rev.* **1995**, *95*, 865. (b) Edelmann, F. T. In *Comprehensive Organometallic Chemistry II*; Abel, E. W., Stone, F. G. A., Wilkinson, G., Eds.; Pergamon: New York, 1995; Vol. 4, p 11.

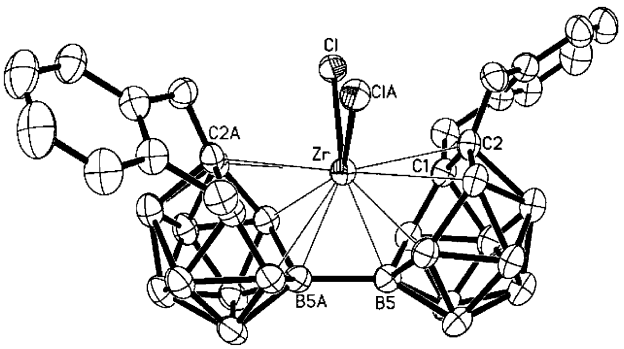

Figure 11. Structure of $\{[o\text{-}C_6H_4(CH_2)_2C_2B_{10}H_9]_2ZrCl_2\}^{2-}$, reproduced by permission of the American Chemical Society from ref 28.

Scheme 12

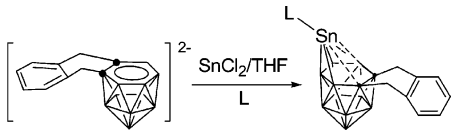

$\{[o\text{-}C_6H_4(CH_2)_2C_2B_{10}H_9]_2ZrCl_2\}\{Na(THF)_3\}_2$ as the minor product, as well as the *o*-carborane μ-1,2-$[o\text{-}C_6H_4(CH_2)_2]$-1,2-$C_2B_{10}H_{10}$ (Scheme 11).[28] The formation of the Zr(II) complex and *o*-carborane can be ascribed to the redox reaction between $ZrCl_4$ and the *nido*-carborane dianion, whereas the isolation of the Zr(IV) complex is unexpected.[28] X-ray diffraction studies showed that the Zr(IV) complex is an *ansa*-zirconocene species with a distorted-tetrahedral geometry, in which the Zr atom is located at a 2-fold axis and σ-bound to two chlorine atoms and η^6-bound to two CAd carboranyl cages that are linked to each other via a B−B bond, as shown in Figure 11. The presence of the B−B bond results in a large variation of the Zr−cage atom distances ranging from 2.455(6) to 2.869(6) Å. The mechanism for the formation of this complex is not clear.[29]

CAd *nido*-carborane ligands can also be incorporated into 13-vertex metallacarboranes of p-block metals and late transition metals. Interaction of $SnCl_2$ with $\{\mu\text{-}7,8\text{-}[o\text{-}C_6H_4(CH_2)_2]\text{-}7,8\text{-}C_2B_{10}H_{10}\}^{2-}$ gave, after recrystallization in donor solvents, the stannacarboranes 4-L-μ-1,2-$\{o\text{-}(CH_2)_2C_6H_4\}$-4,1,2-$SnC_2B_{10}H_{10}$ (L = THF, DME, MeCN) in moderate yield (Scheme 12).[30] X-ray diffraction studies showed that the interaction between the tin atom and carboranyl is very diverse and dependent upon the basicity of the coordinated donor solvents: a stronger base leads to an increased slip distortion of the tin atom from the center of the C_2B_4 bonding face of the carboranyl ligand. Reduction of μ-1,2-$(CH_2)_3$-1,2-$C_2B_{10}H_{10}$ with sodium metal, followed by treatment with metal halides, afforded reasonable yields of the 13-vertex metallacarboranes 4-L-μ-1,2-$(CH_2)_3$-4,1,2-$MC_2B_{10}H_{10}$ (L = Cp, M = Co; L = *p*-cymene, M = Ru; L = $(PMe_2Ph)_2$, M = Pt; L = dppe, M = Ni) (Scheme 13). They were characterized both spectroscopically and crystallographically.[31]

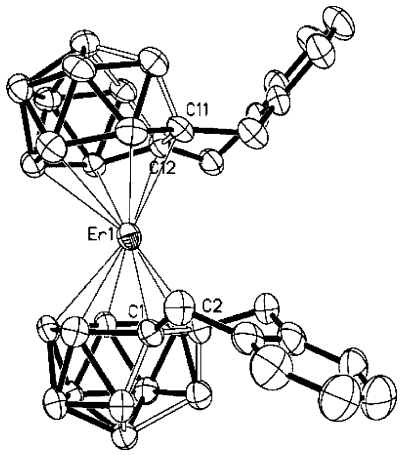

Figure 12. Structure of $\{[\eta^6\text{-}\mu\text{-}1,2\text{-}[o\text{-}C_6H_4(CH_2)_2]\text{-}1,2\text{-}C_2B_{10}H_{10}]_2\text{-}Er\}^{5-}$, reproduced by permission of the American Chemical Society from ref 26.

Scheme 13

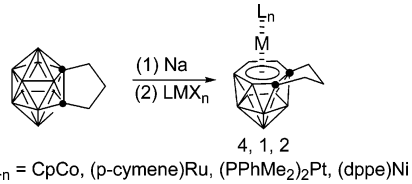

Scheme 14

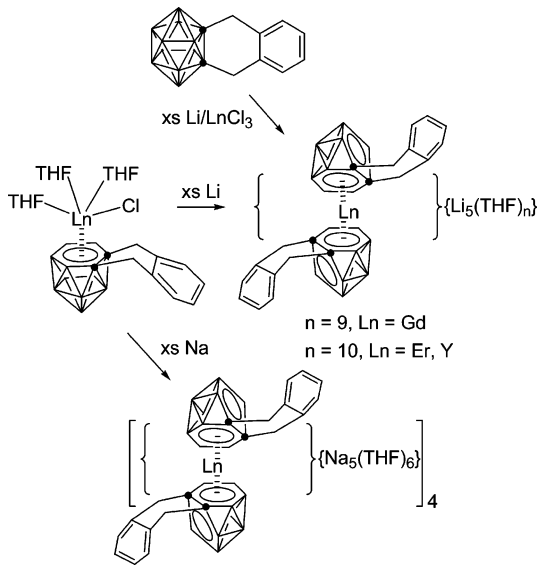

Interaction of the CAd *arachno*-carborane tetraanionic salt $[\{\mu\text{-}1,2\text{-}[o\text{-}C_6H_4(CH_2)_2]\text{-}1,2\text{-}C_2B_{10}H_{10}\}Li_4(THF)_6]_2$ with $LnCl_3$ led to the isolation of the full-sandwich complexes $\{[\eta^6\text{-}\mu\text{-}1,2\text{-}[o\text{-}C_6H_4(CH_2)_2]\text{-}1,2\text{-}C_2B_{10}H_{10}]_2Ln\}\{Li_5(THF)_{10}\}$ (Ln = Er, Y). They were also prepared by either the reaction of μ-1,2-$[o\text{-}C_6H_4\text{-}(CH_2)_2]$-1,2-$C_2B_{10}H_{10}$ with an excess of Li metal in the presence of $LnCl_3$ in THF or treatment of the lanthanacarboranes 4-Cl-4,4,4-$(THF)_3$-μ-1,2-$[o\text{-}C_6H_4(CH_2)_2]$-4,1,2-$LnC_2B_{10}H_{10}$ with an excess of Li metal in THF (Scheme 14).[26] X-ray diffraction studies showed that the complexes consist of the full-sandwich lanthanacarborane moiety $\{[\eta^6\text{-}\mu\text{-}1,2\text{-}[o\text{-}C_6H_4(CH_2)_2]\text{-}1,2\text{-}C_2B_{10}\text{-}H_{10}]_2Ln\}^{5-}$ and five associated complex cations $\{Li(THF)_x\}^+$ which have no bonding interactions with the pentagonal C_2B_3 face. Figure 12 shows the representative structure of the full-sandwich lanthanacarborane moiety $\{[\eta^6\text{-}\mu\text{-}1,2\text{-}[o\text{-}C_6H_4(CH_2)_2]\text{-}1,2\text{-}C_2B_{10}H_{10}]_2Er\}^{5-}$, in which the two hexagonal C_2B_4 bonding

(28) Kwong, W.-C.; Chan, H.-S.; Tang, Y.; Xie, Z. *Organometallics* **2004**, *23*, 3098.

(29) For B-B-linked borane derivatives, see: (a) Su, Y.-X.; Reck, C. E.; Guzei, I. A.; Jordan, R. F. *Organometallics* **2000**, *19*, 4858. (b) Li, F.; Shelly, K.; Kane, R. R.; Knobler, C. B.; Hawthorne, M. F. *J. Am. Chem. Soc.* **1996**, *118*, 6506. (c) Watson-Clark, R. A.; Knobler, C. B.; Hawthorne, M. F. *Inorg. Chem.* **1996**, *35*, 2963.

(30) Wong, K.-H.; Chan, H.-S.; Xie, Z. *Organometallics* **2003**, *22*, 1775.

(31) McIntosh, R.; Ellis, D.; Gil-Lostes, J.; Dalby, K. J.; Rosair, G. M.; Welch, A. J. *Dalton Trans.* **2005**, 1842.

Scheme 15

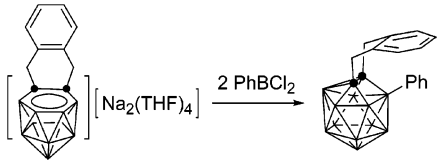

Scheme 16

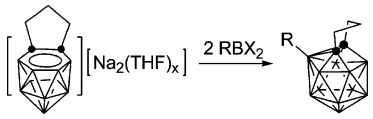

R = H, phenyl, *cis*-1,2-diethylvinyl, *trans*-2-*tert*-butylvinyl

faces are not parallel to each other, rather with a dihedral angle of 20.5°, and the Cent−Er−Cent angle is 152.1°. Excess Na metal can also react with the lanthanacarboranes 4-Cl-4,4,4-(THF)$_3$-μ-1,2-[*o*-$C_6H_4(CH_2)_2$]-4,1,2-$LnC_2B_{10}H_{10}$ to give similar full-sandwich complexes (Scheme 14).[26] It is noteworthy that the open five-membered C_2B_3 ring in these lanthanacarboranes does not bond to lanthanides or group 1 metal ions, presumably due to steric reasons. On the other hand, CAd *arachno*-carborane tetraanions can be readily oxidized by d-block transition-metal halides to the corresponding neutral *o*-carboranes.[32] Therefore, their applications in d-transition metal chemistry have been unsuccessful.

13-Vertex Carboranes

closo-Carboranes having more than 12 vertices (named supercarboranes) are long-sought clusters. The knowledge regarding these molecules has been limited merely to the possible cage geometries predicted by theoretical work.[33] Recent calculations on the boranes $B_nH_n^{2-}$ show that the overall stability of these clusters increases as n gets larger, with the exception of $n = 12$, which is much more stable than the others.[34] Such an "icosahedral barrier" is often used to account for the failure in the syntheses of supercarboranes.[35]

Recognition of the relatively lower reducing power of CAd carborane anions over the CAp counterparts offers a very valuable entry point to the synthesis of supercarboranes. The first 13-vertex carborane, μ-1,2-$C_6H_4(CH_2)_2$-5-Ph-1,2-$C_2B_{11}H_{10}$, was obtained in 6% yield in the reaction of CAd [μ-7,8-C_6H_4-$(CH_2)_2$-7,8-$C_2B_{10}H_{10}$]Na_2 with $PhBCl_2$ (Scheme 15).[36,37] Single-crystal X-ray analyses showed that it adopts a henicosahedral geometry, which is different from the predicted docosahedron of $B_{13}H_{13}^{2-}$.[33] The preference of the henicosahedral structure over the docosahedral structure can be explained by DFT calculations, which revealed that the former is energetically more favorable than the latter.[36] Subsequently, a series of 13-vertex carboranes were synthesized by treatment of the CAd carborane

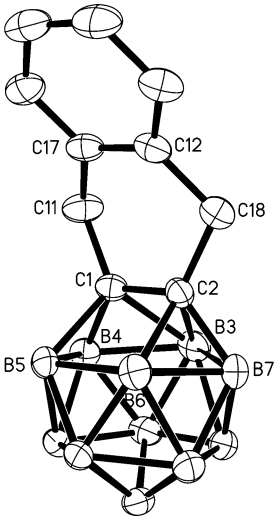

Figure 13. Structure of μ-1,2-[*o*-$C_6H_4(CH_2)_2$]-1,2-$C_2B_{11}H_{11}$, reproduced by permission of the American Chemical Society from ref 38.

Scheme 17

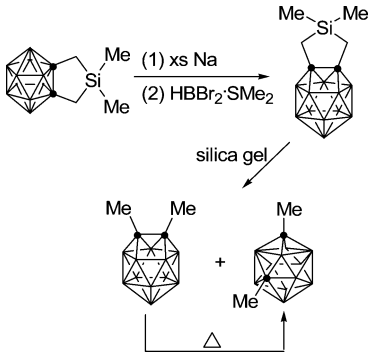

dianionic salt [μ-7,8-$(CH_2)_3$-7,8-$C_2B_{10}H_{10}$]Na_2 with boron dihalides in 7−32% yield, depending upon the substituents on the haloboranes (Scheme 16).[38] In general, less bulky and more electron-rich borane reagents offer higher yields. These 13-vertex carboranes are quite stable in air and soluble in common organic solvents. Figure 13 shows the representative structure of μ-1,2-$C_6H_4(CH_2)_2$-1,2-$C_2B_{11}H_{11}$.[38]

The above 13-vertex carboranes are all CAd species with a C,C′ linkage. Is such a linkage necessary to stabilize the supercarboranes? To study the role of the linkages in the formation and stabilization of 13-vertex carboranes, a 12-vertex carborane with a removable linkage, μ-1,2-$Me_2Si(CH_2)_2$-1,2-$C_2B_{10}H_{10}$,[39] was chosen for this purpose. Reaction of this carborane with an excess of Na metal, followed by treatment with 2 equiv of $HBBr_2$·SMe_2 in toluene, gave the 13-vertex μ-1,2-$Me_2Si(CH_2)_2$-1,2-$C_2B_{11}H_{11}$ in 39% isolated yield. It was subjected to column chromatography on SiO_2, offering the two new 13-vertex carboranes CAd 1,2-Me_2-1,2-$C_2B_{11}H_{11}$ and CAp 1,6-Me_2-1,6-$C_2B_{11}H_{11}$ in 60% and 30% yields, respectively (Scheme 17).[40] The CAd isomer can be quantitatively converted to the thermodynamically more stable 1,6-Me_2-1,6-$C_2B_{11}H_{11}$ upon heating without any decomposition. The molecular structure of 1,2-Me_2-1,2-$C_2B_{11}H_{11}$ has been confirmed by single-crystal X-ray analyses, shown in Figure 14. Its CAp isomer 1,6-

(32) Wong, K.-H. M.Phil. Thesis, The Chinese University of Hong Kong, 2004.
(33) (a) Brown, L. D.; Lipscomb, W. N. *Inorg. Chem.* **1977**, *16*, 2989. (b) Bicerano, J.; Marynick, D. S.; Lipscomb, W. N. *Inorg. Chem.* **1978**, *17*, 2041. (c) Bicerano, J.; Marynick, D. S.; Lipscomb, W. N. *Inorg. Chem.* **1978**, *17*, 3443.
(34) Schleyer, P. v. R.; Najafian, K.; Mebel, A. M. *Inorg. Chem.* **1998**, *37*, 6765.
(35) Grimes, R. N. *Angew. Chem., Int. Ed.* **2003**, *42*, 1198.
(36) Burke, A.; Ellis, D.; Giles, B. T.; Hodson, B. E.; MacGregor, S. A.; Rosair, G. M.; Welch, A. J. *Angew. Chem., Int. Ed.* **2003**, *42*, 225.
(37) Boyd, A. S. F.; Burke, A.; Ellis, D.; Ferrer, D.; Giles, B. T.; Laguna, M. A.; McIntosh, R.; Macgregor, S. A.; Ormsby, D. L.; Rosair, G. M.; Schmidt, F.; Wilson, N. M. M.; Welch, A. J. *Pure Appl. Chem.* **2003**, *75*, 1325.
(38) Deng, L.; Chan, H.-S.; Xie. Z. *J. Am. Chem. Soc.* **2006**, *128*, 5218.
(39) Heying, T. L.; Ager, J. W., Jr.; Clark, S. L.; Alexander, R. P.; Papetti, S.; Reid, J. A.; Trotz, S. I. *Inorg. Chem.* **1963**, *2*, 1097.
(40) Zhang, J.; Deng, L.; Chan, H.-S.; Xie, Z. *J. Am. Chem. Soc.* **2007**, *129*, 18.

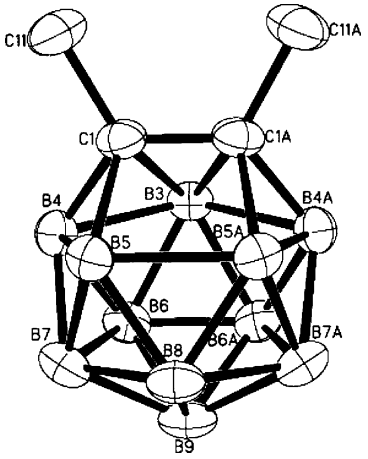

Figure 14. Structure of 1,2-Me_2-1,2-$C_2B_{11}H_{11}$, reproduced by permission of the American Chemical Society from ref 40.

Scheme 18

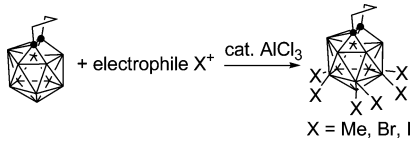

Me_2-1,6-$C_2B_{11}H_{11}$, also prepared by the reaction of CAp [*nido*-7,9-Me_2-7,9-$C_2B_{10}H_{10}$]Na_2 with $HBBr_2$·SMe_2 in 5% yield, is proposed to have a docosahedral structure with all triangulated faces. These results clearly show that the linkages are not necessary for the formation and stabilization of 13-vertex carboranes.[40]

Reactivity studies showed that 13-vertex carboranes can undergo electrophilic substitution reactions. Treatment of μ-1,2-$(CH_2)_3$-1,2-$C_2B_{11}H_{11}$ with an excess of MeI, Br_2, or I_2 in the presence of a catalytic amount of $AlCl_3$ gave the corresponding hexasubstituted 13-vertex carboranes 8,9,10,11,12,13-X_6-μ-1,2-$(CH_2)_3$-1,2-$C_2B_{11}H_5$ (X = Me, Br, I) (Scheme 18).[38] Single-crystal X-ray analysis of the methyl and bromo compounds revealed that the substitution reactions occur at the B−H vertices which are the farthest away from the cage carbons. This result is consistent with that found in *o*-carboranes.[41] Figure 15 shows the representative structure of the hexamethylated 13-vertex carborane. On the other hand, 13-vertex carboranes are found to be less chemically stable than their icosahedral analogues.[38] For example, they can be degraded by H_2O_2 and the hexahalogenated 13-vertex carboranes are hygroscopic. These differences may be ascribed to the joint effects of substituents and the more open trapezoidal faces presented in 13-vertex carboranes.

13-Vertex carboranes can be readily reduced by group 1 and 2 metals to yield the corresponding 13-vertex *nido*-carboranes (Scheme 19).[38] Such a reduction process is much faster than that observed in icosahedral cages and naphthalene is not required, supporting the previous argument that 13-vertex carboranes are more reactive than the 12-vertex species. X-ray diffraction studies showed that the *nido*-carborane dianions in these salts have a bent five-membered open face with the out-of-plane (C(1)C(2)B(3)B(4)) displacement of the B(8) atom ranging from 0.68 to 0.72 Å and with the B(3)···B(4) separation being about 2.64 Å in all structures.[38] The cations in these complexes are not incorporated into the cage but, rather, bind with the peripheral terminal BH moieties via M···H−B bonding interactions, affording exo-nido species. Figure 16 shows the representative structure of the monomeric calcium complex. These 13-vertex *nido*-carborane dianions can be easily oxidized

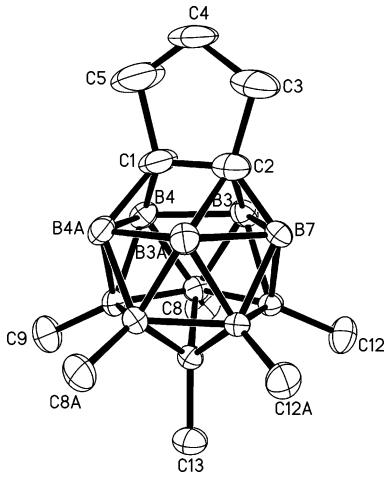

Figure 15. Structure of 8,9,10,11,12,13-$(CH_3)_6$-μ-1,2-$(CH_2)_3$-1,2-$C_2B_{11}H_5$, reproduced by permission of the American Chemical Society from ref 38.

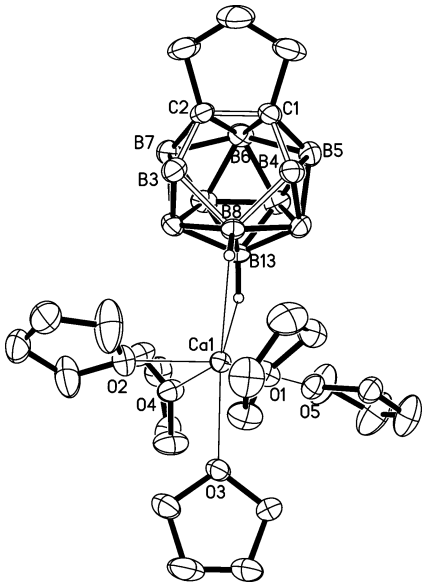

Figure 16. Structure of [{μ-1,2-$(CH_2)_3$-1,2-$C_2B_{11}H_{11}$}{$Ca(THF)_5$}], reproduced by permission of the American Chemical Society from ref 38.

Scheme 19

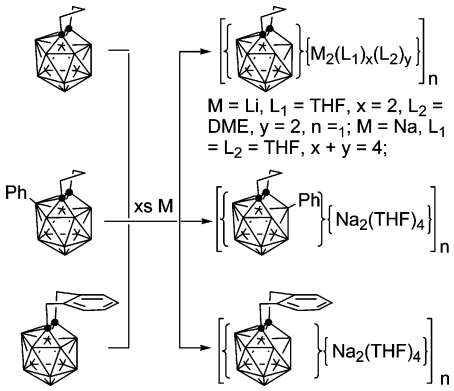

(41) (a) Teixidor, F.; Barberà, G.; Vaca, A.; Kivekäs, R.; Sillanpää, R.; Oliva, J.; Viñas, C. *J. Am. Chem. Soc.* **2005**, *127*, 10158. (b) Potenza, J. A.; Lipscomb, W. N. *Inorg. Chem.* **1966**, *5*, 1483. (c) Vaca, A.; Teixidor, F.; Kivekäs, R.; Sillanpää, R.; Viñas, C. *Dalton Trans.* **2006**, 4884 and references therein.

Scheme 20

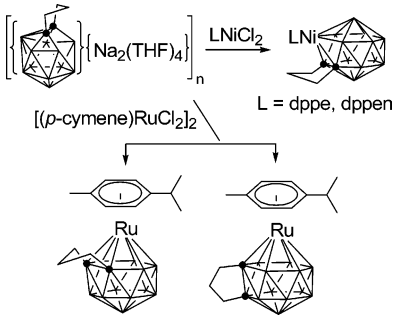

back to closo species by oxygen. In sharp contrast to the CAd 12-vertex *nido*-carboranes, CAd 13-vertex analogues are resistant to further reduction by excess Li metal. As a result, 13-vertex *arachno*-carborane remains elusive.

14-Vertex Metallacarboranes of the MC_2B_{11} System

Group 1 metal salts of 13-vertex *nido*-carborane anions are useful synthons for the production of 14-vertex metallacarboranes. Treatment of CAd *nido*-$[(CH_2)_3C_2B_{11}H_{11}]Na_2$ with $LNiCl_2$ in THF gave the 14-vertex nickelacarboranes $LNi[\eta^5\text{-}(CH_2)_3C_2B_{11}H_{11}]$ (L = 1,2-bis(diphenylphosphino)ethane (dppe), *cis*-1,2-bis(diphenylphosphino)ethene (dppen)) (Scheme 20).[38] X-ray analyses revealed that they adopt a distorted-bicapped-hexagonal-antiprismatic geometry with two seven-coordinate boron vertices, in which the nickel and two cage carbon atoms occupy the 8-, 2-, and 3-positions, respectively, giving 8-L-μ-2,3-$(CH_2)_3$-8,2,3-$NiC_2B_{11}H_{11}$ clusters. The Ni atom is η^5-bound to the bent open face (C(1)C(2)B(3)B(4)B(8)) with a relatively long Ni(1)−B(8) bond distance of ∼2.46 Å, while the other Ni−cage atom distances lie in the range 2.06−2.22 Å. Figure 17 shows the molecular structure of 8-dppe-μ-2,3-$(CH_2)_3$-8,2,3-$NiC_2B_{11}H_{11}$. These 14-vertex nickelacarboranes are much less stable than their 13-vertex analogues.[31,42] Decomposition takes place when they are exposed to air and moisture.

Interaction between CAd *nido*-$[(CH_2)_3C_2B_{11}H_{11}]Na_2$ and $[(p\text{-cymene})RuCl_2]_2$ afforded another class of 14-vertex metallacarboranes, μ-2,3-$(CH_2)_3$-1-(*p*-cymene)-1,2,3-$RuC_2B_{11}H_{11}$ and μ-2,8-$(CH_2)_3$-1-(*p*-cymene)-1,2,8-$RuC_2B_{11}H_{11}$ (Scheme 20).[43,44] As interconversion between the two isomers was not observed, it is suggested that they were formed simultaneously in the capitation step. Different from the case for the nickel species, the 14-vertex ruthenacarboranes are quite air- and moisture-stable. Single-crystal X-ray analyses revealed that they possess a bicapped-hexagonal-antiprismatic geometry. Figure 18 shows the molecular structure of the 1,2,3-isomer, in which the carboranyl is η^6 bound to the ruthenium atom with the Ru−cage atom distances ranging from 2.25 to 2.29 Å. This bonding interaction is very similar to that in μ-1,2-$(CH_2)_3$-4-(*p*-cymene)-4,1,2-$RuC_2B_{10}H_{10}$[31] but is very different from that observed in the 14-vertex nickelacarboranes.[38] Examination of the structures of 13-vertex *nido*-carboranes and these 14-vertex ruthenacarboranes indicates that significant cage rearrangements occur during the reaction. The sizes of the central metal ions may play a role in this process. It is noted that proper selection of the metal salts is crucial for the preparation of stable 14-vertex

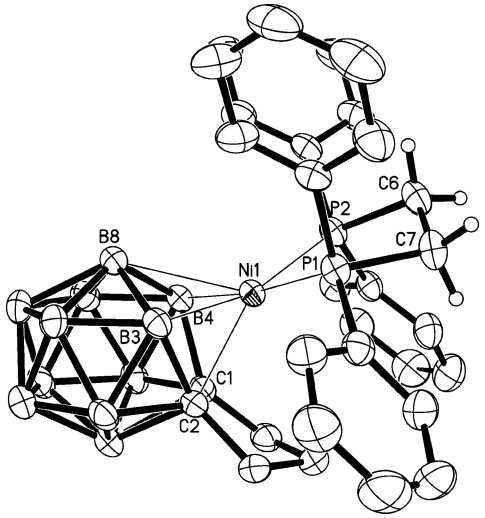

Figure 17. Structure of $[\eta^5\text{-}(CH_2)_3C_2B_{11}H_{11}]Ni(dppe)$, reproduced by permission of the American Chemical Society from ref 38.

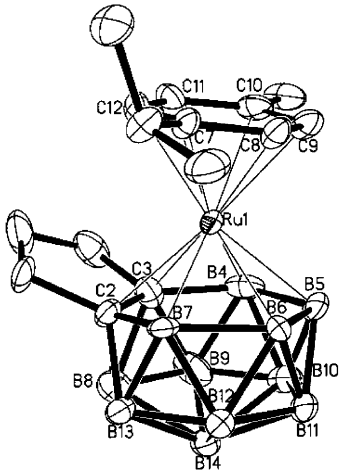

Figure 18. Structure of μ-2,3-$(CH_2)_3$-1-(*p*-cymene)-1,2,3-$RuC_2B_{11}H_{11}$, reproduced by permission of Wiley-VCH from ref 43.

Scheme 21

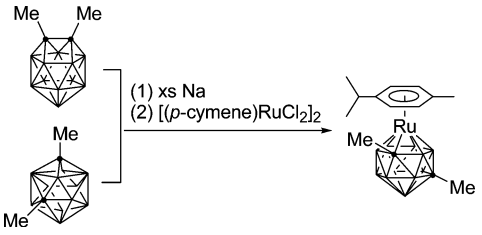

metallacarboranes. For example, only a redox reaction between $SnCl_2$ ($ZrCl_4$ or $(Ph_3P)_2PdCl_2$) and $Na_2[(CH_2)_3C_2B_{11}H_{11}]$ was observed, giving quantitatively μ-1,2-$(CH_2)_3$-1,2-$C_2B_{11}H_{11}$ and metal according to the ^{11}B NMR analyses. On the other hand, a mixture of inseparable products was generated if $(Ph_3P)_2NiCl_2$, $(Ph_3P)_2PtCl_2$, and $(Ph_3P)_3RuCl_2$ were used as starting materials.[38]

Reduction of 1,2-Me_2-1,2-$C_2B_{11}H_{11}$ or 1,6-Me_2-1,6-$C_2B_{11}H_{11}$ with an excess of Na metal in THF afforded two different 13-vertex *nido*-carboranes, respectively, as evidenced by their distinct ^{11}B NMR spectra. Both salts were treated with 0.5 equiv of $[(p\text{-cymene})RuCl_2]_2$ in THF to produce the same CAp 14-vertex ruthenacarborane, 2,9-Me_2-1-(*p*-cymene)-1,2,9-$RuC_2B_{11}H_{11}$, in 19% and 75% yields, respectively (Scheme 21).[40] As shown in Figure 19, it has a geometry similar to that found in the CAd 14-vertex ruthenacarboranes, but the two cage carbons are not

(42) Laguna, M. A.; Ellis, D.; Rosair, G. M.; Welch, A. J. *Inorg. Chim. Acta* **2003**, *347*, 161.
(43) Deng, L.; Zhang, J.; Chan, H.-S.; Xie, Z. *Angew. Chem., Int. Ed.* **2006**, *45*, 4309.
(44) McIntosh, R. D.; Ellis, D.; Rosair, G. M.; Welch, A. J. *Angew. Chem., Int. Ed.* **2006**, *45*, 4313.

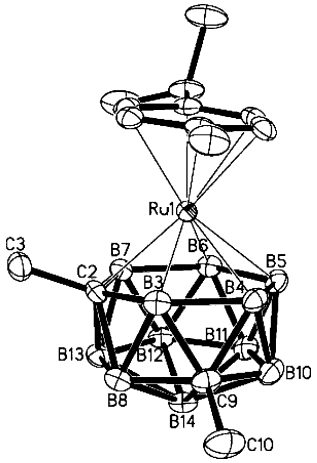

Figure 19. Structure of 2,9-$(CH_3)_2$-1-(*p*-cymene)-1,2,9-$RuC_2B_{11}H_{11}$, reproduced by permission of the American Chemical Society from ref 40.

Scheme 22

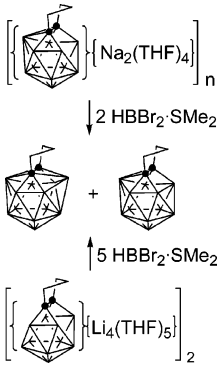

adjacent; rather, they occupy the 2,9-positions, respectively. This result indicates that the cage rearrangements are involved in the reactions, leading to the formation of a thermodynamically more stable product.[40]

14-Vertex Carboranes and 15-Vertex Metallacarboranes

CAd *arachno*-carborane tetraanions have both 6- and 5-membered bonding faces which may take up two $\{BH\}^{2+}$ moieties in one reaction, affording 14-vertex carboranes. Such a [12 + 2] protocol has proved to be successful. Treatment of the 12-vertex CAd *arachno*-carborane tetraanionic salt [{μ-1,2-$(CH_2)_3$-1,2-$C_2B_{10}H_{10}$}{$Li_4(THF)_5$}]$_2$ with 5 equiv of $HBBr_2$·SMe_2 in toluene gave the first 14-vertex carborane, μ-2,3-$(CH_2)_3$-2,3-$C_2B_{12}H_{12}$, in 7% isolated yield. It can also be prepared in much higher yield via a [13 + 1] protocol by the reaction of [{$(CH_2)_3C_2B_{11}H_{11}$}{$Na_2(THF)_4$}]$_n$ with 1.5 equiv of $HBBr_2$·SMe_2 in toluene (Scheme 22).[45] Figure 20 shows the molecular structure of μ-2,3-$(CH_2)_3$-2,3-$C_2B_{12}H_{12}$. It is a bicapped-hexagonal-antiprismatic molecule, with all 24 faces being triangulated. The two 7-coordinate boron atoms in the 1- and 14-positions engender longer B−C and B−B bonds with a distance of ∼1.90 Å.

These cage-expansion methods, which work well in the preparation of 13- and 14-vertex carboranes, have been unsuccessful when applied to the synthesis of 15-vertex carboranes. Reaction of the 14-vertex *closo*-carborane μ-2,3-$(CH_2)_3$-2,3-$C_2B_{12}H_{12}$ with an excess of sodium metal in THF afforded the CAd 14-vertex *nido*-carborane salt [{$(CH_2)_3C_2B_{12}H_{12}$}{$Na_2(THF)_4$}]$_n$ (Scheme 23).[43,45] As shown in Figure 21, the CAd 14-vertex *nido*-carborane cage in this salt has a bent 5-membered open face which is larger and flatter than that observed in the CAd 13-vertex nido species. Similar to the case for the 13-vertex CAd *nido*-carboranes, this 14-vertex *nido*-carborane is also resistant to further reduction by an excess of Li metal. Treatment of [{$(CH_2)_3C_2B_{12}H_{12}$}{$Na_2(THF)_4$}]$_n$ with $HBBr_2$·SMe_2 in toluene generated an isomer of 14-vertex carborane, μ-2,8-$(CH_2)_3$-2,8-$C_2B_{12}H_{12}$. No 15-vertex carborane was detected, after many attempts. This sodium salt can be oxidized by oxygen to give μ-2,8-$(CH_2)_3$-2,8-$C_2B_{12}H_{12}$ (Scheme 23).[43] X-ray analysis revealed that the two cage carbon atoms occupy the 2,8-positions, respectively, with a C(cage)−C(cage) bond distance of 1.599(3) Å, which is very close to the 1.608(4) Å observed in its 2,3-isomer. Both isomers reacted with Na metal to produce the same 14-vertex CAd *nido*-carborane, $[(CH_2)_3C_2B_{12}H_{12}]^{2-}$, as indicated by ^{11}B NMR spectra (Scheme 23).[45]

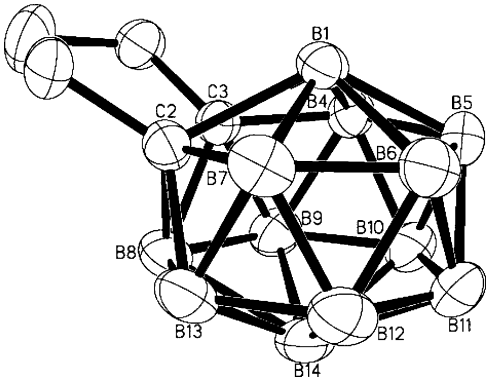

Figure 20. Structure of μ-2,3-$(CH_2)_3$-2,3-$C_2B_{12}H_{12}$, reproduced by permission of Wiley-VCH from ref 43.

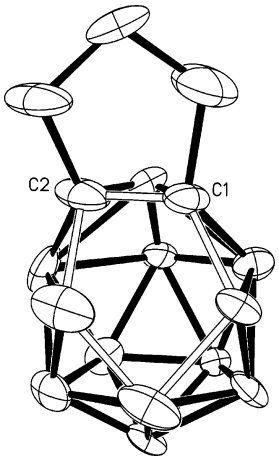

Figure 21. Structure of $[(CH_2)_3C_2B_{12}H_{12}]^{2-}$, reproduced by permission of Wiley-VCH from ref 43.

Scheme 23

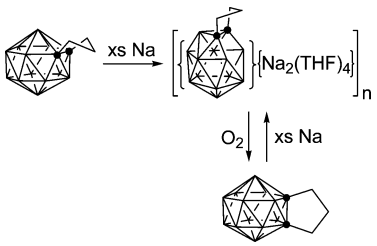

(45) Deng, L.; Chan, H.-S.; Xie, Z. *Angew. Chem., Int. Ed.* **2005**, *44*, 2128.

Scheme 24

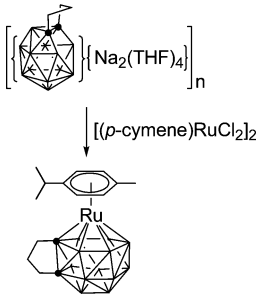

Scheme 25

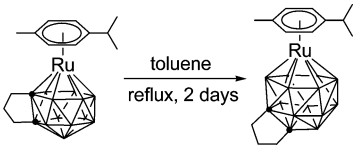

Although the preparation of a 15-vertex carborane has been unsuccessful using the cage-opening and boron insertion methodologies, a metal fragment can be incorporated into the 14-vertex *nido*-carborane to give a 15-vertex metallacarborane. Interaction of the 14-vertex *nido*-carborane salt $Na_2[(CH_2)_3C_2B_{12}H_{12}]$ with $[(p\text{-cymene})RuCl_2]_2$ afforded the 15-vertex metallacarborane μ-1,4-$(CH_2)_3$-7-(p-cymene)-7,1,4-$RuC_2B_{12}H_{12}$ in 62% yield (Scheme 24).[43] It is an air- and moisture-stable complex. An X-ray analysis revealed that this 15-vertex metallacarborane adapts a closo structure bearing 26 triangulated faces and has an approximate D_{3h} symmetry, omitting the tethering group and the differences among the Ru, B, and C atoms. This geometry is very similar to that predicted for $B_{15}H_{15}^{2-}$ by theoretical calculations.[33] In this mixed-sandwich molecule (Figure 22), the arene ring is parallel to the hexagonal bonding face (C(4)B(2)B(5)B(10)B(12)B(15)) of the carborane ligand with an average Ru−cage atom distance of 2.247(3) Å and an average Ru−C(ring) distance of 2.272(3) Å. Careful examination of the structures of the nido species and the 15-vertex metallacarborane clearly indicates that significant cage rearrangements occur during the reaction. Another 15-vertex ruthenacarborane, μ-1,6-$(CH_2)_3$-7-(*p*-cymene)-7,1,6-$RuC_2B_{12}H_{12}$, was prepared by the thermolysis of the 14-vertex ruthenacarborane μ-2,8-$(CH_2)_3$-1-(*p*-cymene)-1,2,8-$RuC_2B_{11}H_{11}$ (Scheme 25).[44] It is suggested that the formation of this 15-vertex species may involve adventitious capture of a {BH} fragment. These 15-vertex ruthenacarboranes represent the largest *closo*-heteroborane clusters known thus far.

Conclusions and Perspectives

With the assistance of a transition-metal ion, the CAp *nido*-carboranes $[nido\text{-}7,9\text{-}R_2\text{-}7,9\text{-}C_2B_{10}H_{10}]^{2-}$ can be further reduced by group 1 metals to give CAp *arachno*-carboranes $[arachno\text{-}R_2C_2B_{10}H_{10}]^{4-}$. The geometries of the arachno species are dependent upon the electronic configurations of the transition-metal ions: a boat shape with one open seven-membered ring for the metal ions with d^0/f^n configurations and a hexagonal antiprism for the metal ions with d^n configurations. On the other hand, the CAd *arachno*-carboranes $[arachno\text{-}1,2\text{-}R'_2\text{-}1,2\text{-}C_2B_{10}H_{10}]^{4-}$ can be prepared by the direct reaction of CAd *nido*-carboranes $[nido\text{-}7,8\text{-}R'_2\text{-}7,8\text{-}C_2B_{10}H_{10}]^{2-}$ with Li metal in the absence of any transition-metal ions. They have a basket shape with one open hexagonal and one open pentagonal face that share a common edge of the C(cage)−C(cage) bond.

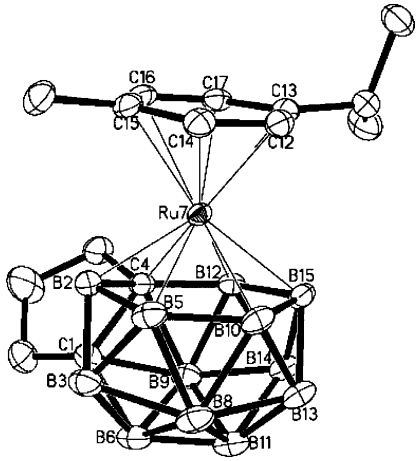

Figure 22. Structure of μ-1,4-$(CH_2)_3$-7-(*p*-cymene)-7,1,4-$RuC_2B_{12}H_{12}$, reproduced by permission of Wiley-VCH from ref 43.

Controlled synthesis of CAp and CAd *nido*-carborane dianions can be achieved by tuning the length/rigidity of the carbon chains between the two cage carbon atoms. A short linkage can thus force the two cage carbons in adjacent positions during the reduction, leading to the formation of CAd *nido*-carborane dianions. As they can be further reduced by Li metal to generate the corresponding CAd *arachno*-carboranes, whereas the CAp *nido*-carboranes are inert to Li metal in the absence of transition-metal ions, it is therefore suggested that CAd *nido*-carboranes are weaker reducing agents (or stronger oxidants) than their CAp counterparts. This result provides a very valuable entry point to the synthesis of 13-vertex carboranes. Accordingly, a new class of both CAd and CAp 13-vertex carboranes was prepared. CAp 13-vertex carboranes are thermodynamically more stable than their CAd counterparts. These results suggest that the C,C′ linkage between the two cage carbons has no obvious effect on the formation and stabilization of 13-vertex carboranes. A 14-vertex carborane was subsequently prepared via the [12 + 2] protocol by the reaction of CAd *arachno*-carborane with boron dihalide reagents.

Both 13- and 14-vertex carboranes are more reactive than their icosahedral analogues. They can be readily reduced by group 1 metals to the corresponding 13- and 14-vertex *nido*-carboranes, which are resistant to further reduction by Li metal. Thus, both 13- and 14-vertex *arachno*-carboranes remain elusive. Because of the very strong reducing power of the 14-vertex *nido*-carborane, the boron-insertion reaction is prohibited, which makes the synthesis of a 15-vertex carborane unfeasible using the cage-opening and boron-insertion methods. On the other hand, both 13- and 14-vertex *nido*-carboranes are useful synthons for the production of 14- and 15-vertex metallacarboranes.

Since the cluster sizes of metallacarboranes are in principle controlled by those of carboranes, carboranes with more than 14 vertices have become new synthetic targets. To achieve this goal, new borane reagents with lower oxidizing power are needed to prevent the redox reactions between *nido*-carborane dianions and borane reagents, thus facilitating the capitation reactions. New synthetic methodologies such as the convergent [12 + *n*] (*n* > 2) approach await development. As the research in supercarboranes becomes more active, a new class of boron clusters of extraordinary size and unique structures can be envisaged. The search for applications of these superclusters in many disciplines such as BNCT, electronics, catalysis, polymers, and nanomaterials is anticipated in the future.

Acknowledgment. We thank the Research Grants Council of the Hong Kong Special Administration Region and The Chinese University of Hong Kong for financial support over the years. We are grateful to our collaborators with whom we have had the pleasure to interact. We also thank Professor Dietmar Seyferth for his kind invitation and editing of this article.

OM061053D